Proceedings World Geothermal Congress 2026
Calgary, Canada, June 8 – 11, 2026

Mapping Radiogenic Heat Production in the Horn River Basin, Northeast British Columbia, Canada, Using Geophysical Well Log Data

Kezhen Hu[1]*, Stephen E. Grasby[1] and Xiaojun Liu[1]
[1] Natural Resources Canada, Geological Survey of Canada-Calgary
*kezhen.hu@nrcan-rncan.gc.ca

Keywords: Radiogenic heat production; Geophysical well logs; the Horn River Basin

1. INTRODUCTION

Radiogenic heat production (RHP) is a critical component of the subsurface thermal regime, with direct implications for petroleum system modeling, reservoir quality, and geothermal energy potential (Beardsmore & Cull, 2001). This heat is predominantly generated by the radioactive decay of isotopes of uranium (U), thorium (Th), and potassium (K), contributing significantly to the thermal structure of sedimentary basins. Crustal heat production can vary widely, ranging from less than 0.1 $\mu W/m^3$ in mafic rocks to more than 6 $\mu W/m^3$ in granites (e.g., Rybach, 1976). Conventional models of hot sedimentary aquifer geothermal systems typically assume that heat originates primarily from the crystalline basement, composed of igneous and metamorphic rocks, while the overlying sedimentary strata are generally viewed as passive thermal insulators with minimal intrinsic heat generation. However, recent studies have shown that sedimentary rocks, particularly organic-rich shales, can also contribute significantly to RHP, especially in regions where these rocks have high concentrations of uranium, thorium, and potassium (e.g., Hasterok et al., 2018). Moreover, measured RHP values in shales range from 2 to 6.42 $\mu W/m^3$, potentially matching or even exceeding those of basement rocks in some regions (e.g., Batista-Rodriguez et al., 2023). In thick, laterally extensive formations, radiogenic sediments can generate substantial internal heat and elevate geothermal gradients and subsurface temperatures, reducing dependence on basement-derived heat (Majorowicz & Grasby, 2021).

Within the Western Canadian Sedimentary Basin (WCSB), northeastern British Columbia (NEBC) is characterized by elevated basement radiogenic heat production (AGS, 1994). High-RHP sedimentary units have also been identified, such as the Exshaw shale (e.g., Bachu & Burwash, 1991). Notably, the Horn River Basin in NEBC is distinguished by its extensive shale gas development, abundant well data, high thermal gradients, and elevated uranium concentrations in certain formations, which together make it a promising target for geothermal exploration (Hu et al., 2022; Majorowicz & Grasby, 2021; Palmer-Wilson et al., 2018).

This study examines the RHP in sedimentary formations of the Horn River Basin, with a focus on the organic-rich Horn River Group shale near the base of the basin. By integrating bottom-hole temperature data with geophysical well logs, the spatial variability of U, Th, and K concentrations is evaluated. The resulting RHP values are correlated with gamma ray logs, and their spatial distribution across the basin is mapped to assess their contribution to the regional thermal regime.

2. GEOLOGICAL SETTINGS

The Horn River Basin (HRB), located north of Fort Nelson near the British Columbia–Northwest Territories border, Canada (Fig. 1a), hosts substantial energy resources, including both unconventional gas and geothermal potential within the Devonian-age Horn River Group (HRG). The HRG is composed predominantly of organic-rich, fine-grained marine shales and is subdivided into three formations, from base to top: Evie, Otter Park, and Muskwa (Fig. 1b).

The Evie Formation, which unconformably overlies the Lower Keg River carbonates, comprises dark gray to black, organic-rich, pyritic, and variably calcareous to siliceous shale. It represents the most radioactive interval within the HRB and contains the highest total organic carbon (TOC) content among the HRG formations (e.g., Hu et al., 2022). The overlying Otter Park Formation consists of more clay-rich, calcareous shales with lower TOC and increased ductility. Above this, the Muskwa Formation conformably underlies the Fort Simpson Formation and is composed of gray to black, siliceous, organic-rich shale. The HRG is thermally mature to overmature across the basin, making it a key target for shale gas development (e.g., Dong et al., 2017; Rivard et al., 2014). Its thermal maturity reflects variations in burial depth and heat flow, with the region characterized by relatively high geothermal gradients (e.g., Majorowicz & Grasby, 2021).

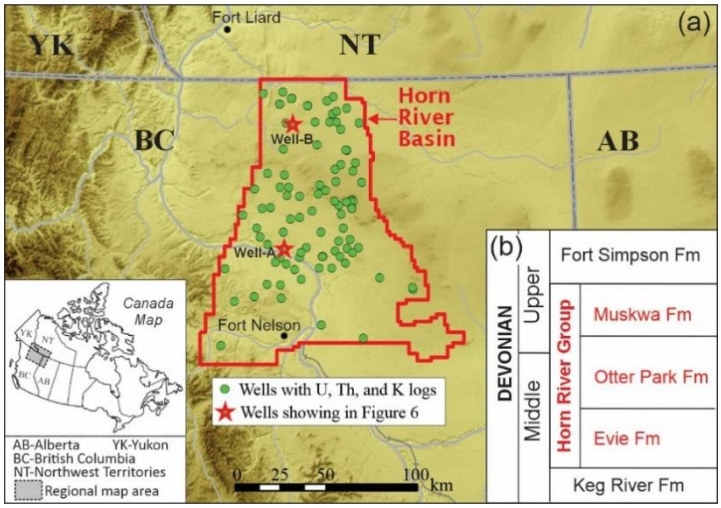


Figure 1. (a) Modified Digital Elevation Map showing the location of the study area and the vertical wells where spectral gamma ray log set is available. The original DEM/Hillshade is derived from the Canadian Digital Elevation Model, Color Shaded Relief (CDEM, 2023). (b) Schematic stratigraphic chart of the Horn River Group in the Horn River Basin.

3. DATA AND METHODS

Spectral gamma ray (SGR) logging detects gamma radiation from naturally occurring isotopes—uranium (U), thorium (Th), and potassium (K)—by measuring their characteristic energy spectra. Unlike conventional gamma ray logs that record only total radiation, SGR logs quantify the individual concentrations of U, Th, and K, enabling more detailed lithological characterization and geochemical interpretation. For this study, we analyzed SGR data from 84 wells (Fig. 1a), including total gamma ray and individual U, Th, and K logs. In addition, conventional logs from over 160 wells were integrated, comprising natural gamma ray (GR), compressional sonic transit time, bulk density, deep resistivity, photoelectric factor (where available), and density/neutron porosity. Bottom-hole temperature (BHT) data from over 200 wells were also included.

Radiogenic heat production was calculated for subsurface formations using radioactive elemental concentrations from SGR logs. These RHP values were then correlated with GR logs through regression analysis to develop a new GR-based model for predicting RHP in wells lacking elemental logs, specifically across the HRG formations: Muskwa, Otter Park, and Evie. RHP values derived from both elemental and GR logs were interpolated using geostatistical methods to generate continuous distribution maps. A comparative analysis of the three formations was conducted to evaluate their relative contributions to regional radiogenic heat production. To complement the RHP assessment, thermal gradient profiles were also constructed.

RHP (*A*) was calculated using the method originally proposed by Rybach (1976) and later refined by Bücker and Rybach (1996), which relates RHP to U, Th, and K concentrations and incorporates bulk density:

$$A1 = 10^{-5} RHOB\ (9.52\ Cu + 2.56\ CTh + 3.48\ Ck) \quad (1)$$

where A1 is the RHP calculated using Eq. 1 (μW/m^3). RHOB is the bulk density (kg/m^3), and Cu, CTh, Ck are the concentrations of U (ppm), Th (ppm), and K (%), respectively.

RHP (A2) was estimated from GR log using an empirical linear regression by Bücker and Rybach (1996):

$$A2 = 0.0158\ (GR - 0.8) \quad (2)$$

where A2 is the RHP calculated only from GR log (in API units) using Equation 2.

This study establishes a relationship between A1 and GR data for the HRG shales, expressed as:

$$A3 = \mathrm{a}\ GR + b \quad (3)$$

where A3 is the RHP calculated using Equation 3, representing the GR model proposed in this study, and a and b are constants obtained by fitting the GR log data to the calculated A1 values for the HRG formations.

4. RESULTS AND DISCUSSION

Continuous SGR logs reveal distinct log signatures within the HRG shale. Figure 2a-d shows the basin-wide distribution of SGR log data (GR, U, Th, K) for the three formations, which form the basis for the RHP calculations. The Evie Formation displays the highest GR and U readings but the lowest Th and K values, while the Otter Park

Formation has the lowest SGR and U readings but the highest Th and K. The Muskwa Formation exhibits intermediate values across all four log types.

In this study, BHT data, primarily from well tests such as production and drill stem tests (DSTs), indicate that temperatures in the HRG shales typically range from 80 to 155 °C (Fig. 2e), with an average geothermal gradient of 46.4 °C /km, confirming the high thermal gradient of the region.

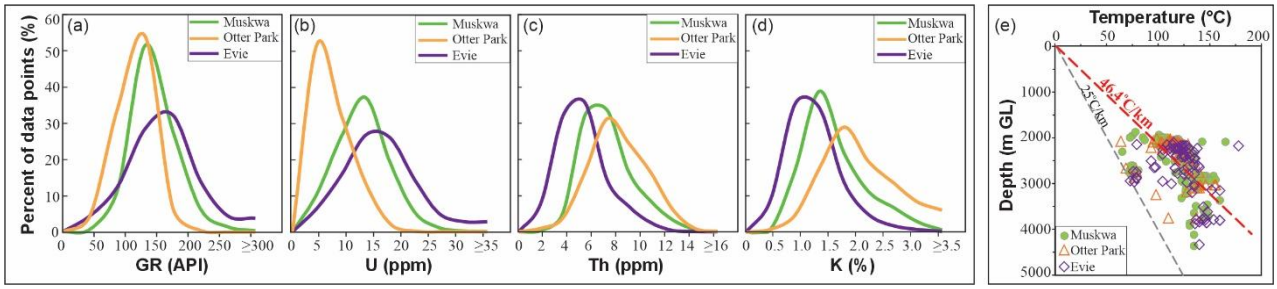


Figure 2. SGR logs highlighting the distinct features of GR (a), U (b), Th (c), and K (d) across the Muskwa, Otter Park, and Evie formations. (e) BHT data from 231 wells that penetrated the HRG in the HRB.

Applying Equation 1, RHP (A1) was directly calculated from U, Th, K, and RHOB logs in all wells with available SGR logs across the HRB, revealing a wide range of values from 0.2 to 12.91 μW/m^3. Figure 3 shows the A1 distribution across the three formations: the Muskwa Formation ranges from 0.41 to 8.81 μW/m^3, with an average of 3.6 μW/m^3 (Fig. 3a); the Otter Park Formation shows lower values, ranging from 0.2 to 7.84 μW/m^3, averaging 2.3 μW/m^3 (Fig. 3b); and the Evie Formation exhibits a broader range from 0.24-12.91 μW/m^3, with an average of 4.3 μW/m^3 (Fig. 3c).

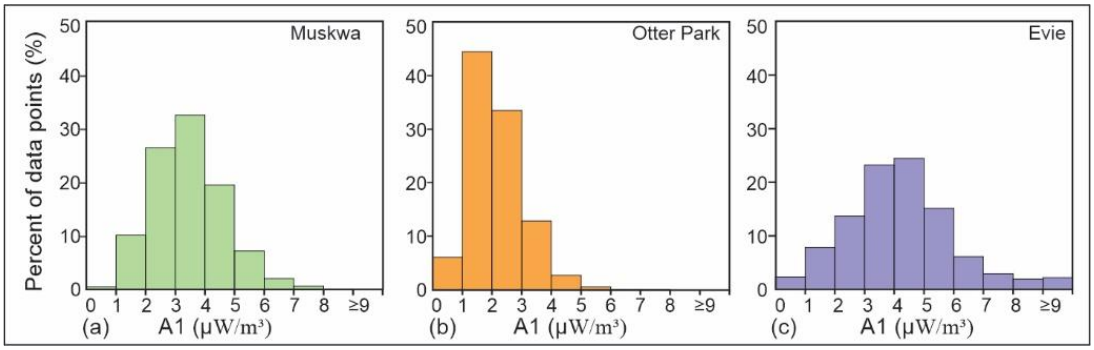


Figure 3. Distributions of calculated RHP (A1) from radioactive elemental logs using Equation 1 for the three formations within the HRG shale: (a) Muskwa, (b) Otter Park, and (c) Evie.

By correlating A1 with GR logs, Equation 3 was derived in this study (Fig. 4), illustrating the relationship between RHP (A1) and GR logs for the HRG shale (Fig. 4a) and for each of the three formations (Fig. 4b-d).

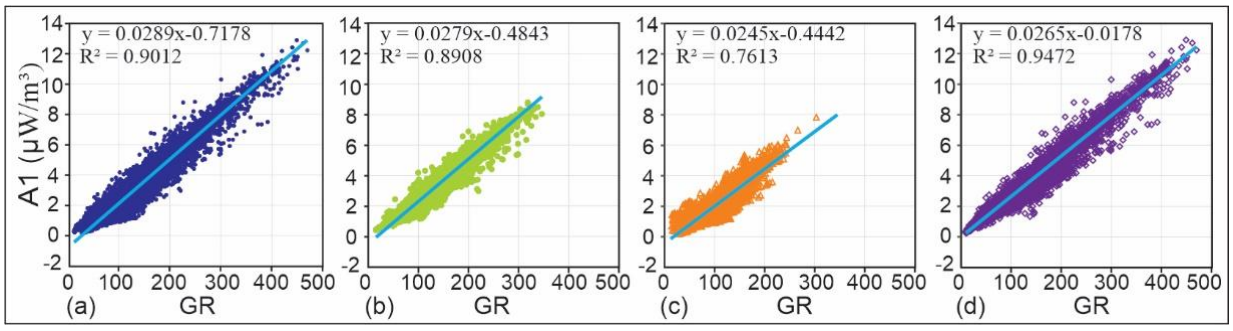


Figure 4. Correlations between A1 (calculated using Equation 1) and total gamma ray (GR) logs for the HRG (a), Muskwa Formation (b), Otter Park Formation (c), and Evie Formation (d).

Accordingly, A2 and A3 were estimated from GR log using Equations 2 and 3, respectively. To validate the GR-based models, Figure 5 compares their estimates (A2, A3) against the SGR-derived baseline (A1). The published GR model (Equation 2) shows high fidelity only at low RHP values (0~2 μW/m^3; Fig. 5a), where higher Th/U ratios (>1.8) are also observed (Fig. 5b). However, A2 tends to significantly underestimate RHP in the HRG shales at higher values (>2 μW/m^3) (Fig. 5a), with the discrepancy increasing as Th/U ratio decreases and/or RHP increases (Fig. 5b). In contrast, the improved GR model (Equation 3) accurately predicts RHP across the full range (Fig. 5c), allowing reliable estimates for wells lacking SGR logs in the HRB.

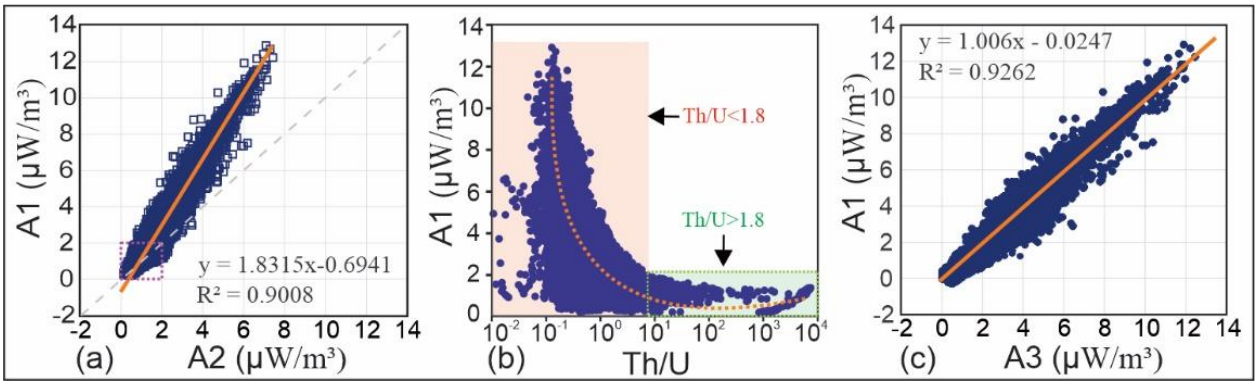


Figure 5. (a) Correlation between A1 (calculated using Equation 1) and A2 (derived from Equation 2); (b) relationship between A1 and the thorium to uranium (Th/U) ratio; and (c) comparison of A1 with A3 (derived from the improved GR model, Equation 3, proposed in this study).

Figure 6 illustrates RHP calculation for two example wells (Well-A and Well-B; Fig. 1). In Well-A (Fig. 6a), the composite log suite includes SGR logging set (tracks 1-2), conventional well logs (tracks 3-5), and continuous RHP profiles: A1 (from radioactive elemental logs), A2 (from the published GR model, Eq. 2); and A3 (from the improved GR model, Eq. 3). All three RHP curves exhibit similar trends, with A3 closely matching A1. Although the published GR model (A2, Eq. 2) provides estimates comparable to A1 at low RHP values (<2 μW/m^3), it increasingly underestimates RHP at higher values (>2 μW/m^3), with the discrepancy widening as RHP increases. In Well-B (Fig. 6b), where radioactive elemental logs are absent, RHP was calculated using both GR models. A pronounced discrepancy between A2 and A3 is observed across the HRG section, particularly in the Evie Formation, where the maximum RHP exceeds 10 μW/m^3 and Equation 2 substantially underestimates RHP.

Within the HRG in both wells, the Evie Formation shows the highest RHP, reaching or exceeding 10 μW/m^3, attributed to elevated uranium content and/or high GR readings. The Otter Park Formation displays the lowest RHP, while the Muskwa Formation exhibits intermediate values.

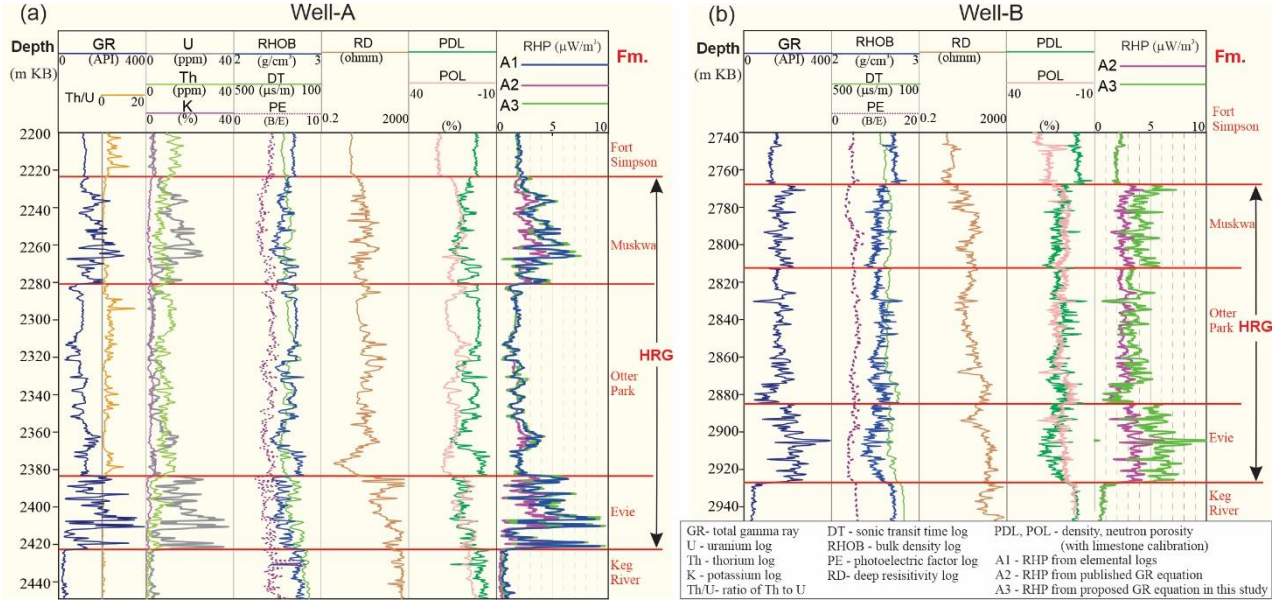


Figure 6. RHP calculations from well logs for two example wells. (a) Well-A (central well in Fig. 1) with SGR logs (tracks 1–2), showing three RHP logs (track 6) derived from both elemental and GR logs; (b) Well-B (northern well in Fig. 1), lacking elemental logs, showing two RHP logs derived solely from GR logs.

Consequently, RHP was estimated using the proposed GR model (Eq. 3) for wells lacking elemental logs. Contour maps were then generated (Fig. 7) to illustrate the spatial distribution of calculated RHP across the HRG formations within the HRB. In the Muskwa Formation (Fig. 7a), RHP values primarily range from 3 to 4 μW/m^3, with relatively higher values broadly distributed throughout the basin, except in the central-south portion. The Otter Park Formation (Fig. 7b) shows RHP values mainly between 2 and 3 μW/m^3, with higher concentrations in the northern part of the basin and lower values towards south. The Evie Formation (Fig. 7c) exhibits generally higher RHP, predominantly ranging from 4 to 5 μW/m^3, with zones of elevated RHP (> 5 μW/m^3) extending from the northwest to southeast and occurring locally in the southwestern part of the basin.

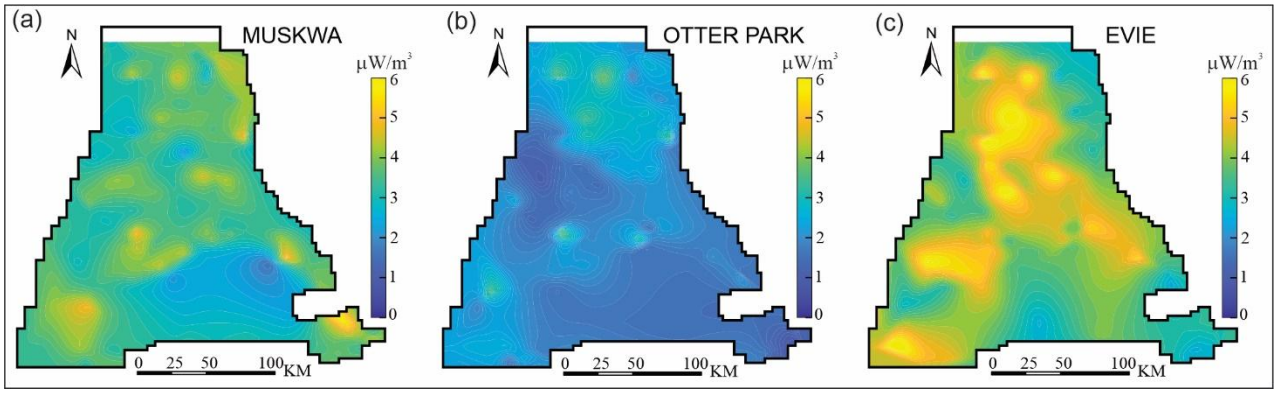


Figure 7. Contour maps of RHP calculated from radioactive elemental and/or GR logs using Equations 1 and 3 for the three formations within the HRG shale: (a) Muskwa, (b) Otter Park, and (c) Evie.

5. CONCLUSIONS

This study quantifies RHP in the HRG shale of the HRB using geophysical well logs. RHP was calculated from density and radioactive elemental logs (RHOB, U, Th, K) in wells with SGR data. Building on these results and regression analysis, a new GR-based model was developed to estimate RHP in wells lacking SGR logs. The model yields results consistent with those derived from elemental logs and highlights the underestimation of RHP by the published GR model at higher RHP values (>2 μW/m^3). Using RHP values from both the element-based model and the improved GR model, regional distributions of average RHP were mapped for the HRG formations. Results reveal significant variability across the basin: the Evie Formation exhibits the highest average RHP (4.3 μW/m^3), the Otter Park Formation the lowest (2.3 μW/m^3), and the Muskwa Formation falls in between (3.6 μW/m^3). Elevated RHP, particularly values exceeding 4 μW/m^3 in the Evie Formation near the base of the HRB, indicates substantial internal heat generation. When integrated with BHT data and regional basement heat production (AGS, 1994), our results indicate that RHP from the HRG shale contributes significantly to the total basin-wide thermal regime, accounting for up to 40%. This also implies that, in the absence of this radiogenic shale, the Horn River Basin might be less thermally mature, which has important implications for oil and gas generation.

Acknowledgements

This project is part of the GeoEnergy Program with Natural Resources Canada (NRCan), Geological Survey of Canada, and financial support was provided through the Office of Energy Research and Development (OERD), NRCan. Well log data were provided by the British Columbia Oil and Gas Commission.

REFERENCES

AGS-Alberta Geological Survey (1994). Atlas of the Western Canada Sedimentary Basin (1994), Chapter 30- Geothermal Regime : https://ags.aer.ca/publications/atlas-western-canada-sedimentary-basin/chapter-30-geothermal-regime

Bachu, S. & Burwash, R.A. (1991). Regional-scale analysis of the geothermal regime in the Western Canada Sedimentary Basin. Geothermics, 20(5-6), (1991) 387-407. https://doi.org/10.1016/0375-6505(91) 90028-T

Batista-Rodríguez, J.A. et al. (2023). Radiogenic heat production in rocks from the Sabinas Basin (northeastern Mexico) determined by in situ gamma radiation measurements. Environmental Earth Sciences 82.19 (2023): 458.

Beardsmore, G. R. & Cull, J.P. (2001). Crustal Heat Flow: A Guide to Measurement and Modelling. Cambridge University Press. (2001) ISBN: 0521797039

Bucker, C. & Rybach, L. (1996). A simple method to determine heat production from gamma-ray logs. Marine and Petroleum Geology, vol.13, no. 4 (1996) 373–377. https://doi.org/10.1016/0264-8172(95)00089-5

Canadian Digital Elevation Model, Color Shaded Relief (2023). https://open.canada.ca/data/en/dataset/7f245e4d-76c2-4caa-951a-45d1d2051333/resource/a5abf023-f9b8-438a-acf4-f25f24df41d4

Dong, T., Harris, N.B., Ayranci, K. (2017). Twemlow, C.E., Nassichuk, B.R.: The impact of composition on pore throat size and permeability in high maturity shales: Middle and Upper Devonian Horn River Group, northeastern British Columbia, Canada. Marine and Petroleum Geology, vol. 81, (2017) 220–236. https://doi.org/10.1016/j.marpetgeo.2017.01.011

Hasterok, D., Gard, M., Webb, J. (2018). On the radiogenic heat production of metamorphic, igneous, and sedimentary rocks. Geoscience Frontiers 9 (2018) 1777. https://www.sciencedirect.com/science/article/pii/S1674987117301937

Hu, K., Chen, Z., Grasby, S.E. (2022). Compilation and analyses of Horn River Group data from petroleum exploration wells in the Horn River Basin, northeast British Columbia, Canada; Geological Survey of Canada, Open File 8866, 20 p. https://doi.org/10.4095/329622

Majorowicz, J. & Grasby, S. E. (2021). Deep geothermal heating potential for the communities of the Western Canadian Sedimentary Basin. Energies, (2021) 14(3), 706. https://doi.org/10.3390/en14030706

Palmer-Wilson, K., Walsh, W., Banks, J., Wild, P. (2018). Techno-Economic assessment of Geothermal Energy Resources in the Sedimentary Basin in Northeastern British Columbia, Canada. Geoscience BC Report 2018-18.

Rivard, C., Lavoie, D., Lefebvre, R., Séjourne, S., Lamonagne, C., Duchesne, M. (2014). An overview of Canadian shale gas production and environmental concerns. International Journal of Coal Geology, (2014) 126, 64e76. https://doi.org/10.1016/j.coal.2013.12.004

Rybach, L. (1976). Radioactive heat production in rocks and its relation to other petrophysical parameters. Pure and Applied Geophysics, 114(1), 1976, 309–318. https://doi.org/10.1007/BF00878955